Qifeng Shu*, Zhen Wang and Kuochih Chou

Liquidus Temperature of Mould Fluxes in Casting of Ti-stablized Stainless Steel

Abstract: Liquidus temperatures of mould fluxes for casting of Ti-stabilized stainless steel were determined by differential thermal analysis (DTA) techniques in the present work. Multiple DTA curves were employed to guarantee better accuracy for liquidus temperature determination. To investigate effect of compositions change on solidification of mould fluxes during casting of Ti-stabilized stainless steel, changes of liquidus and solidus temperatures with TiO_2 substitution for SiO_2 in mould fluxes were studied. It was found that TiO_2 substitution for SiO_2 in mould fluxes would lead to decrease of liquidus temperature. Thermodynamic package FactSage was also employed to calculate the liquidus temperature of mould fluxes. The calculated results were compared with experimental data, and discrepancy between calculated and experimental liquidus temperatures was discussed.

Keywords: mould fluxes, liquidus temperature, differential thermal analysis, Ti-stabilized stainless steel, FactSage

PACS® (2010). 05.70.±a

***Corresponding author: Qifeng Shu:** School of Metallurgical and Ecological engineering and State Key Laboratory of Advanced Metallurgy, University of Science and Technology Beijing, Beijing 10083, China. E-mail: shuqifeng@gmail.com

Zhen Wang, Kuochih Chou: School of Metallurgical and Ecological engineering and State Key Laboratory of Advanced Metallurgy, University of Science and Technology Beijing, Beijing 10083, China

1 Introduction

Mould fluxes play an important role in continuous casting operation [1]. The major functions of mould fluxes are: (1) protecting steel from oxidation; (2) providing thermal insulation of steel; (3) Absorbing inclusions in steel; (4) providing lubricity between mould and steel shell; (5) Control on the horizon heat transfer. The latter two functions are key functions of mould fluxes for successful casting operation.

In continuous casting practice, mould fluxes are fed on the top of liquid steel pool and form liquid layer. Liquid slags infiltrates into gap between steel and mould. A part of liquid slag solidifies to form solid slag layer, and rest part form a liquid film to lubricate the steel shell. The solid slag layer controls the horizontal heat transfer between mould and shell. The thickness of solid and liquid is essential to functions of lubricity and heat transfer control. At present, thickness of solid slag film are often characterized by breaking temperature, below which there is a marked increase of viscosity [2]. However, breaking temperature is determined in non-equilibrium state and is affected by cooling rates and viscosity measurement conditions. The liquidus temperature would be a better quantity in theoretical consideration.

The casting of Ti-stablized stainless steel would bring many difficulties [3]. One of the most important difficulties is the pickup of TiO_2 in mould slags. The major reason is that titanium in steel could be oxidized by SiO_2 in mould powder to form TiO_2 and cause an increase of TiO_2 concentration in mould fluxes [4] and possible reaction is represented as: $[Ti] + (SiO_2) = [Si] + (TiO_2)$. The increase of TiO_2 concentration in molten mould fluxes could lead to the change of many properties of mould fluxes, e.g. viscosity, liquidus temperature and crystallization behavior. There are some reports [5–10] regarding the effect of TiO_2 concentration on the viscosity, solidification temperature and crystallization. However, these studies were performed to investigate the TiO_2 effect on mould fluxes at fix basicity (defined as CaO/SiO_2). While during process of oxidation reaction, the basicity should increase with the decrease of SiO_2. Therefore, investigation on the substitution of TiO_2 for SiO_2 in mould fluxes would be more beneficial to the industrial practice.

Thermodynamics databases, such as FactSage [11], Thermo-Calc [12] have been extensively applied in process metallurgy. FactSage package has been employed to study the crystallization product of mould fluxes in casting of Ti-stabilized stainless steel [9]. However, due to scarcity of experimental data in slag system bearing fluoride, the accuracy of data generated by thermodynamic software package is questionable. Application of commercial thermodynamic package in study of mould fluxes need to be testified using experimental data.

In the present work, the liquidus temperatures of mould fluxes were determined by differential thermal analysis (DTA) techniques. The effect of TiO_2 substitution for SiO_2 in mould fluxes on liquidus temperature was

investigated. FactSage thermodynamic package was also employed to calculate the liquidus temperature of mould fluxes. The calculated results were compared with experimental data.

2 Experimental

2.1 Sample preparation

The raw materials for preparation of mould fluxes were analytical grade TiO_2, SiO_2, MgO, Al_2O_3, Na_2CO_3, $CaCO_3$ and CaF_2 (Purity of all reagent >99%). Na_2CO_3 and $CaCO_3$ were substitutes for Na_2O and CaO due to their stability in air.

Premelted samples with different compositions were prepared by conventional melting and quenching method. Raw materials were well mixed in mortar, and then taken into a platinum crucible. Melting was carried out in a Muffle furnace at approximately 1573 K in air atmosphere. The samples were held at the setting temperature for nearly 2 h to make sure complete melting and homogenization. Thereafter, melts were quenched by dipping sample into water and bulk glassy samples were formed. Chemical compositions of the pre-melted slag samples were analyzed using X-ray fluorescence spectroscopy (XRF-1800 from Shimadzu) before the DTA measurements. The nominal chemical compositions of the slag and measured chemical composition of the premelted slags are presented in Table 1. It could be seen that measured chemical composition of premelted slags is in consistence with nominal chemical composition of premelted slags except concentrations of CaO and CaF_2, which could be due to accuracy of XRF measurements for F element or HF evaporation. Measured compositions of the present samples by XRF were adopted in the present work. All these glass samples are proved to be amorphous by X-Ray diffraction. Powder X-ray diffraction measurements were carried out on a M21X-SRA X-ray diffractometer (MAC Science) equipped with graphite crystal monchromator in air. The XRD patterns were collected with Cu-Kα radiation.

2.2 Differential thermal analysis

The glass samples were pulverized into powder (150~200 mesh) for differential thermal analysis (DTA). Differential thermal analyses and thermogravimetry (TG) were performed on the glass powder samples at the range of 373~1473 K using differential thermal analyzer (Model: Netzsch STA 449C, Germany) at different heating rate (10 K/min, 20 K/min and 30 K/min) in argon atmosphere. Al_2O_3 was adopted as a reference material. Temperature for DTA was calibrated using the melting points of the high purity substances and an internal calibration file was established.

2.3 Thermodynamic calculation

Liquidus temperature of mould fluxes was calculated in the present work using FactSage databases (version 6.2). The thermodynamics of slag phase was described by a modified quasichemical model proposed by Pelton et al. [11]. The newest version (6.2) of FactSage compound and solution database, FTOxide, contains data for pure oxides and oxide solutions of 20 elements as well as for dilute solutions of S, SO_4, PO_4, H_2O/OH, CO_3, F, Cl, I in the molten slag phase, therefore can provide a comprehensive thermodynamic description for slag phase. The "Equilib" module provides the functions of multi-phase equilibrium calculation using Gibbs energy minimization routine.

3 Results and discussion

Fig. 1 shows DTA curves of samples with TiO_2 concentration of 0%, 5% and 10% at different heating rates of

Table 1: Chemical composition of the studied mould fluxes

Sample no.		Composition (wt.%)						
		CaO	SiO_2	Al_2O_3	MgO	Na_2O	CaF_2	TiO_2
1	Nominal	30.5	38	6	1.5	10	14	0
	Measured	32.63	38.39	6.54	1.48	10.8	10.16	0
2	Nominal	30.5	33	6	1.5	10	14	5
	Measured	35.53	31.06	6.41	1.67	10.44	9.19	5.7
3	Nominal	30.5	28	6	1.5	10	14	10
	Measured	32.5	28.58	6.83	1.61	10.43	9.17	10.87

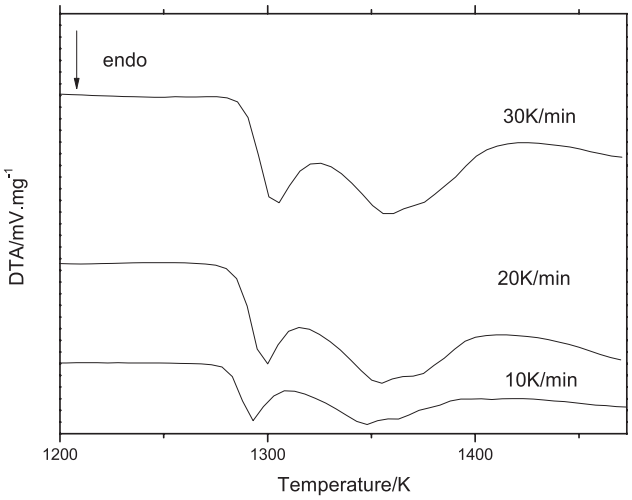

(a)

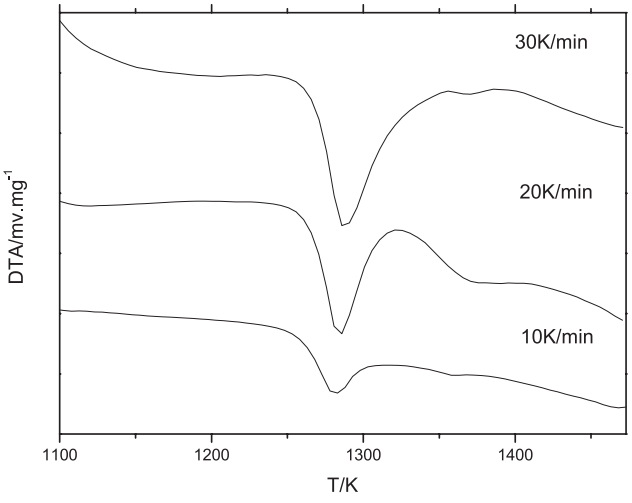

(b)

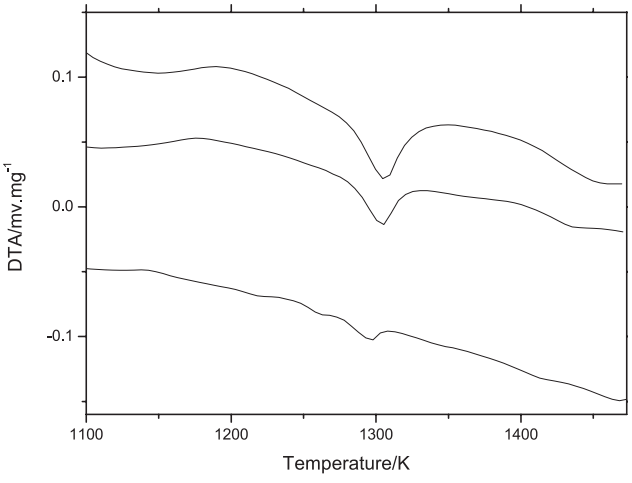

(c)

Fig. 1: DTA curves at different heating rates: (a) sample 1, (b) sample 2, (c) sample 3

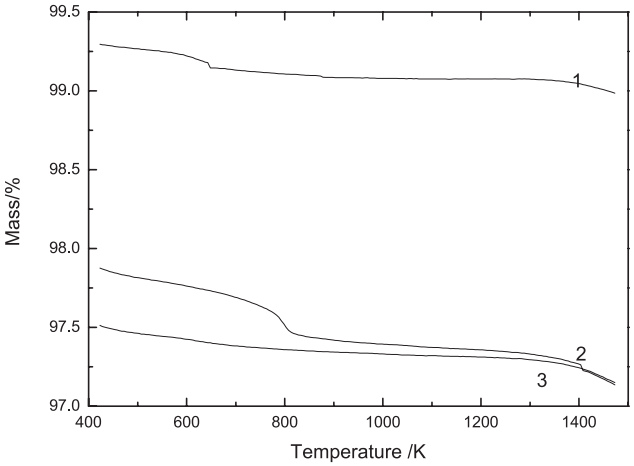

Fig. 2: TG curves at heat rate of 10 K/min for different samples

10 K/min, 20 K/min and 30 K/min. There are several endothermic peaks found in DTA curves from 1073 K to 1473 K, which corresponding the melting process of samples. Fig. 2 shows TG curves of samples with TiO_2 concentration of 0%, 5% and 10% at 10 K/min. It could be found in Fig. 2 that overall weight loss during TG-DTA measurements is less than 1% for all samples, which indicates that evaporation during TG-DTA measurements is negligible. It was found by many researchers that strong supercooling effect was associated with liquidus temperature determination by cooling DTA [13]. Therefore, heating curves were employed in the present study for determination of liquidus temperature. Moreover, glassy samples were adopted to obtain better chemical homogenization of samples. According to our previous study [14] on crystallization of the same samples, glassy samples undergo glass transition and crystallization of cuspidine and $CaTiO_3$ before melting. In order to determine phases during melting process, sample 2 was heated at 1403 K for 20 minutes, then subject to XRD analysis. XRD pattern (Fig. 3) showed that main phases were amorphous phase, cuspidine and perovskite. Therefore, endothermic peaks at present DTA curves could be attributed to melting of cuspidine and perovskite for TiO_2 containing samples.

Fig. 4 illustrated the method to determine solidus and liquidus temperature from a single DTA curve according to suggestion from Boettinger et al. [13]. Solidus temperatures of all samples are determined as the onset temperature of the first peak in DTA curves. As shown in Fig. 4, onset temperature is taken as the intersection of a linear fit to the downward sloping linear section of the peak and extrapolation of the baseline. The last thermal peak temperature is set as the liquidus temperature.

As can be seen in Fig. 1(a), two apparent endothermic peaks corresponding to heat effect due to melting of

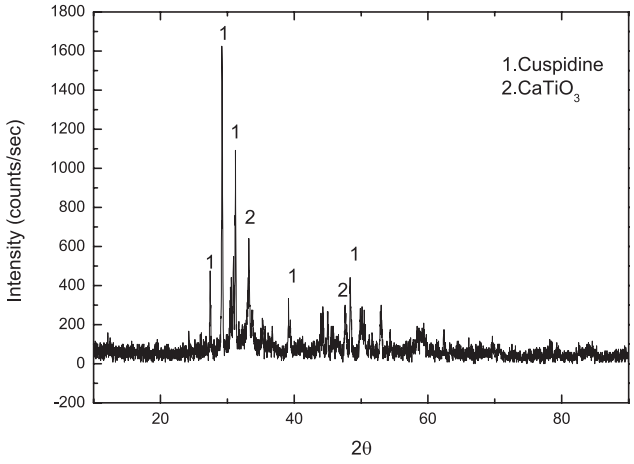

Fig. 3: XRD pattern for sample 2 heating at 1347 K for 20 min

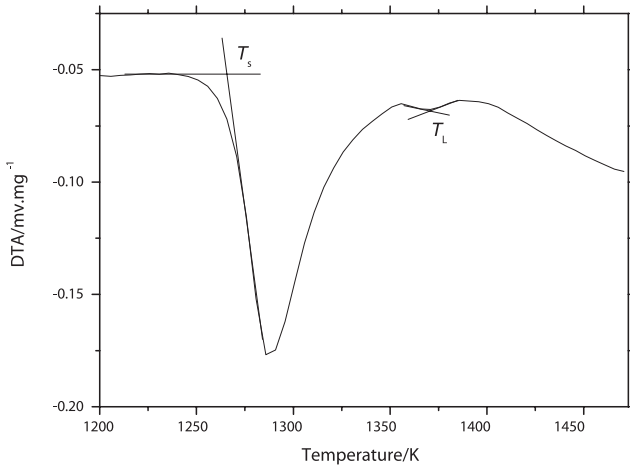

Fig. 4: Example for determination of liquidus and solidus temperature (DTA curve for sample 2 at 30 K/min)

sample could be found in DTA curves. After carefully observation, the second peak could be composed of two close peaks. Thereafter, the peak temperature of last peak would be designated as liquidus temperature for sample without TiO_2. It could be seen from Fig. 1(b) that there appear two endothermic peaks due to melting of sample. liquidus temperature was determined as peak temperature of the second peak. It can be seen in Fig. 1(c) that there is only one endothermic peak in DTA curves of sample 3, as solidus temperature of sample 3 is very close to liquidus temperature.

Fig. 5 shows that determined liquidus temperature of three samples varied with different heating rates. It is well known that liquidus temperatures determined by heating or cooling DTA curves changes with heating or cooling rates [13]. During heating, peaks for determination of liquidus temperature move to high temperature with increase of heating rates. Many works on determination of liquidus temperature were performed at a single heating or cooling rate of 10 K/min or 5 K/min [15]. This would bring some uncertainty on measured values. In the present work, liquidus temperatures for various samples were determined by using multiple DTA curves. It is assumed that a linear correlation exists between liquidus temperature and heating rate, and then relationship between determined liquidus temperatures and heating rate was established by fitting the curves. Since liquidus temperature is a thermodynamic quantity in equilibrium that could only be reached at infinite small heating or cooling rate. Liquidus temperatures were determined by extrapolation to heating rates of 10 K/min. Linear correlations between liquidus temperature and heating rate for samples investigated can be obtained by fitting the curves as follows:

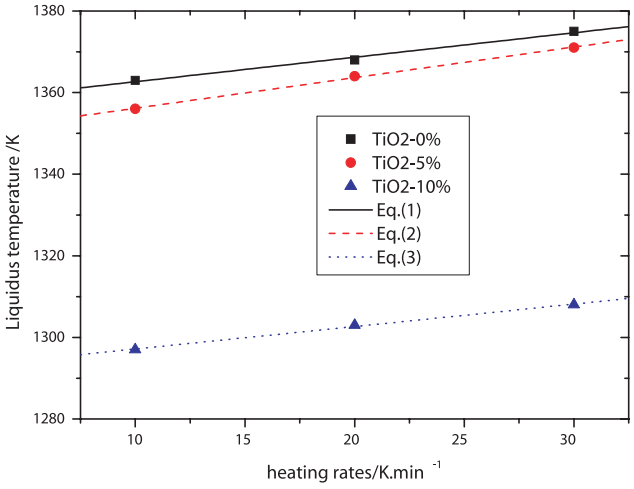

Fig. 5: Liquidus temperatures as functions of heating rates for samples

Sample 1 $T_L = 1357 + 0.60\beta$ (1)

Sample 2 $T_L = 1349 + 0.75\beta$ (2)

Sample 3 $T_L = 1292 + 0.55\beta$ (3)

where T_L is liquidus temperature in (K), β is heating rate in K/min.

As shown in Fig. 6, solidus temperature also increased with increase of heating rates. Linear correlations between solidus temperature and heating rate for samples investigated was also established as follows:

Sample 1 $T_S = 1274 + 0.45\beta$ (4)

Sample 2 $T_S = 1262 + 0.15\beta$ (5)

Sample 3 $T_S = 1271 + 0.15\beta$ (6)

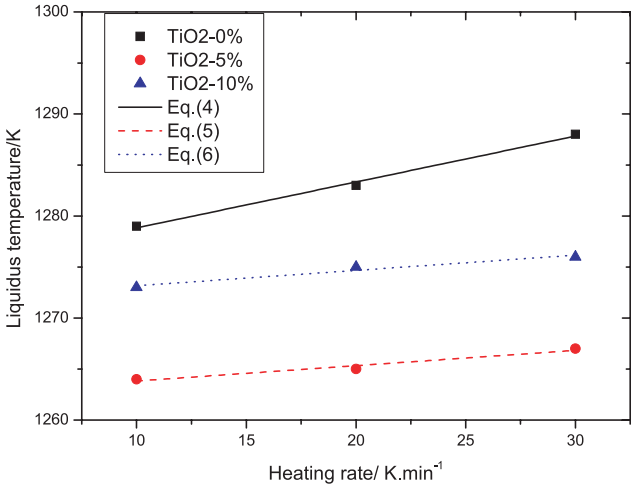

Fig. 6: Solidus temperatures as functions of heating rates for samples

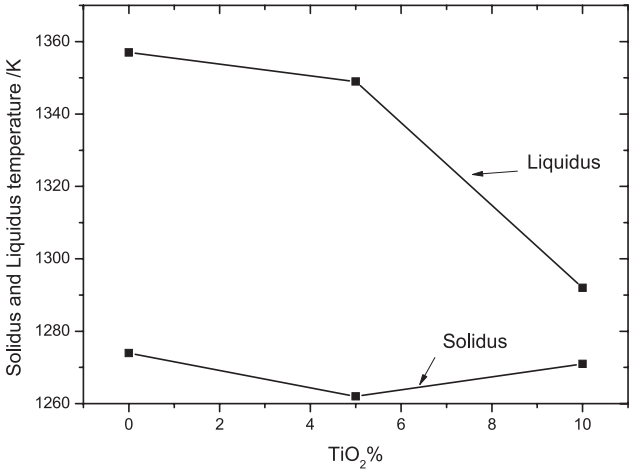

Fig. 7: Liquidus and solidus temperature as a function of concentration of TiO_2 in mould fluxes

Liquidus temperatures at zero heating rate were determined by extrapolation according to Eqs. (1) to (3) Determined Solidus and liquidus temperatures. Fig. 7 show liquidus temperatures and solidus temperatures of slag samples as functions of TiO_2 content in slags. It could be seen that liquidus temperature decrease with increase of TiO_2. Hao et al. [5–6] investigated the solidification temperature of mould fluxes in stainless steel casting with addition of TiO_2 using cooling DTA curves. They found that solidification temperature decreases with increase of TiO_2 concentration in slags. Despite the difference in slag composition and analytical technique, the present result is in consistence with their observation. Sun et al. [10] determined breaking temperature of slags with additions of TiO_2 and found that breaking temperature of slags increases gradually and then increase sharply with increase of TiO_2. Breaking temperature became minimum with 10% TiO_2 addition. Since the maximum TiO_2 content in the present work is 10%, our result is also consistent with theirs. It could be also seen that solidus temperature remains almost the same as TiO_2 increases.

Table 2: Comparison between measured and calculated liquidus temperature

Sample no.	Experimental liquidus temperature (K)	Calculated liquid temperature by FactSage (K)
1	1357	1635
2	1349	1582
3	1292	1530

There are many empirical correlations to calculate the solidification, breaking temperature and liquidus temperature of mould fluxes reported in literature [16]. One correlation for liquidus temperature of mould fluxes is as follow

$$T_{liq}(\mathrm{K}) = 1191 + 11.4\%SiO_2 - 11.0\%CaO + 4.2\%Al_2O_3 + 5.7\%MgO - 10.1\%Na_2O - 15.8\%K_2O + 1.9\%F + 8.3\%Fe_2O_3 + 11.6\%MnO + 273 \quad (7)$$

It would be interesting to compare our measured liquidus temperature with calculated liquidus temperature, solidification temperature or breaking temperature. However, this correlation does not include TiO_2 as a component in their equation. Thereby, calculations were only made in sample 1 free of TiO_2. Calculated liquidus temperature by Eq. (7) is 1399 K, while our measured liquidus temperature is 1357 K. The deviation is about 42 K, which is almost the same as deviation claimed (35 K) by the author [16].

A linear regression on liquidus temperature ~ TiO_2% curve provides a slope of –5.9 K/%TiO_2. Combining Eq. (7) with the present work, a correlation which takes TiO_2 into consideration could be obtained as follows:

$$T_{liq}(\mathrm{K}) = 1191 + 11.4\%SiO_2 - 11.0\%CaO + 4.2\%Al_2O_3 + 5.7\%MgO - 10.1\%Na_2O - 15.8\%K_2O - 5.9\%TiO_2 + 1.9\%F + 8.3\%Fe_2O_3 + 11.6\%MnO + 273 \quad (8)$$

The liquidus temperatures of the samples were also calculated with FactSage thermodynamic software package. FTOxide solution and compound databases are employed in the present study. The comparison between the experimental liquidus temperature data and the calculated values is shown in Table 1. It could be seen that calculated liquidus temperature decreases with increase

of TiO_2 content, which is in line with the present measurements. However, there exists a large discrepancy between experimental liquidus temperature data and the calculated values using FTOxide databases. The largest difference could be more than 200 K. This large discrepancy could be attributed that slag systems containing fluoride are not well optimized in the FToxide database for lacking experimental phase equilibria data.

4 Conclusion

Multiple DTA measurements at different heating rates were performed to determine solidus and liquidus temperature of mould fluxes in the present work. Linear correlations between liquidus temperature and heating rate for samples investigated were established. As content of TiO_2 in mould fluxes increases, liquidus temperature of mould fluxes decreases. A thermodynamic package, FactSage, was also employed to calculated liquidus temperature of mould fluxes. Liquidus temperatures calculated by FactSage package show similar changes with content of TiO_2, however, a large discrepancy between calculated values with measured values exists.

Acknowledgments: The financial supports from NSFC (No. 51174018, 50704002) and research funding for metallurgy of university of science and technology Beijing (YJ2011-003) are gratefully acknowledged.

Received: June 21, 2012. Accepted: March 18, 2013.

References

[1] K.C. Mills and A.B. Fox, *ISIJ Int.*, 2003, 43: 1479.
[2] S. Sridhar, K.C. Mills, O. Afrange, H.P. Lorz and R. Carli, *Ironmaking Steelmaking*, 2000, 27: 238.
[3] T. Kishi, H. Tsubio, H. Takeuchi, T. Nakano, M. Yamamiya and T. Ando, *Nippon Steel Technical Rep.*, 1987, 34: 11.
[4] P.R. Scheller, *Steel Res. Int.*, 2010, 81: 886.
[5] Z.Q. Hao, W.Q. Chen and C. Lippold, *Metall. Mater. Trans. B*, 2010, 41: 805.
[6] Z.Q. Hao, W.Q. Chen, C. Lippold and H.X. Mao, *Chin. J. Process Eng.* (in Chinese), 2009, 9: 514.
[7] T. Mukongo, P.C. Pistorius and A.M. Garbers-Craig, *Ironmaking Steelmaking*, 2004, 31: 135.
[8] H. Todoroki, T. Ishii, K. Mizuno and A. Hongo, *Mater. Sci. Eng., A*, 2005, 121: 413–414.
[9] J.A. Bothma and P.C. Pistorius, *Ironmaking Steelmaking*, 2007, 34: 513.
[10] Lifeng Sun, Hongpo Wang, Maofa Jiang, Qizeng Lin, Chunlai Liu and Yong Zou, *Adv. Mater. Res*., 2011, 107: 189–193.
[11] C.W. Bale, E. Bélisle and P. Chartrand, *Calphad*, 2009, 33: 295.
[12] Bo Sundman, Bo Jansson and Jan-Olof Andersson, The Thermo-Calc databank system, *Calphad*, 1985, 9: 153.
[13] W.J. Boettinger, U.R. Kattner, K.-W. Moon and J.H. Perepezko, DTA and Heat-Flux DSC Measurements of Alloy Melting and Freezing, Methods for Phase Diagram Determination, edited by J.-C. Zhao, Amsterdam, Elsevier, 2007, 181.
[14] Z. Wang, Q.F. Shu, X.M. Hou and K.C. Chou, *Ironmaking and Steelmaking*, 2012, 39: 210–215.
[15] J. Lapsa, B. Onderka, C. Schmetterer, H. Ipser, Y. Yuan and G. Borzone, *Thermochim. Acta*, 2011, 519: 55.
[16] K.C. Mills, A.B. Fox, Z. Li and R.P. Thackray, *Ironmaking Steelmaking*, 2005, 32: 26.